Scientific Research Publishing

Journal of Materials Science and Chemical Engineering, 2024, 12, 33-53
https://www.scirp.org/journal/msce
ISSN Online: 2327-6053
ISSN Print: 2327-6045

Ablation Rates in Limestone Cave Walls or Monuments Linked to Bat Guano

—From *In Situ* Measurements in the Azé Cave (Monts du Mâconnais, France) to Laboratory Modelling

Lionel Barriquand[1*], Vasile Heresanu[2], Olivier Grauby[2], Philippe Audra[3], Laurent Bruxelles[4], Didier Cailhol[4]

[1]Savoie-Mont-Blanc University, Edytem, Le Bourget-du-Lac Cedex, France
[2]Aix-Marseille University-CNRS, CINaM, Campus de Luminy, Marseille, France
[3]Polytech'Lab, University Côte d'Azur, Nice, France
[4]Laboratory TRACES, Université Toulouse Jean Jaurès Maison, Toulouse, France
Email: *lionel.barriquand@wanadoo.fr, Philippe.AUDRA@univ-cotedazur.fr

How to cite this paper: Barriquand, L., Heresanu, V., Grauby, O., Audra, P., Bruxelles, L. and Cailhol, D. (2024) Ablation Rates in Limestone Cave Walls or Monuments Linked to Bat Guano. *Journal of Materials Science and Chemical Engineering*, **12**, 33-53.
https://doi.org/10.4236/msce.2024.1212003

Received: October 7, 2024
Accepted: December 8, 2024
Published: December 11, 2024

Abstract

In caves and monuments, biocorrosion caused by bats occurs partly under accumulations of guano. Tests were carried out both at cave temperature and under hot conditions in the laboratory on 4 different limestones. A comparison of the results obtained using these two methods shows that the processes leading to the weathering of the limestones are the same, and that the hot laboratory tests accelerate them in a well-constrained way. The higher the porosity and capillarity of the limestone, the faster the weathering process. The presence of large calcite crystals also favors weathering. In caves, the ablation rates obtained (8 mm/ka) are sufficient to destroy engravings in a few decades. In monuments, ablation rates are even higher because of the temperature, and could theoretically reach 32 cm/ka in extreme conditions at 80˚C. The laboratory test developed here can be adapted to the temperature of each case study. It has already demonstrated the mechanisms that lead from weathering to the formation of a phosphate crust.

Keywords

Limestone Biocorrosion, Ablation Rate, Karst, Monument Conservation, Phosphatisation

1. Introduction

Caves are natural complexes which, after their initial stage of phreatic formation, evolve over time according to the environmental parameters to which they are subjected (installation of specific ecosystems, changes in climate). These changes result in morphological modifications, both to the walls and along the passages. These are the result of a variety of weathering phenomena.

In terms of archaeology, caves are essential to our knowledge of prehistoric societies and cultures, and for the environmental changes that occurred during the Pleistocene and Holocene periods. While part of the archaeological heritage is buried in the cave sediments, cave art can most often be seen on the walls, in sections of galleries or chambers that have been more or less degraded by environmental changes since they were created. As a result, the remains of prehistoric art that have come down to us have necessarily benefited from special protective conditions, which have enabled them to be preserved in a small number of caves, in particular the occlusion of the entrances, which has isolated them from the climatic and biological influences of the surface: Lascaux Cave [1], Cosquer Cave [2] [3], Chauvet Cave [4] [5], Coliboaia Cave [6]. Generally speaking, they are most often described as caves of karstic origin that are considered to be "fossil" and therefore inactive. With new concepts being considered, it is now necessary to re-read underground landscapes using criteria other than those usually used for the formation of epigenic caves developed by underground flows made aggressive by the carbonic acid of vegetation.

To this end, the various methodologies applied to karstic caves enable a more precise approach to the description and understanding of underground landscapes. Above all, they offer a different perspective and a fresh look at the study and conservation of cave art.

As a result of the multidisciplinary approach to the study of karst caves developed over the last few decades, it is now possible to integrate these new processes. These are environmental in nature, such as the climatology of the cave and the identification of past and present ecosystems. The role of biotic factors in geochemical phenomena highlights the dynamics of active processes involved in the evolution of cave morphologies. Recent research in karstology has shown the importance of late-stage weathering of cave walls. Some of this weathering is of biological origin, known as "biocorrosion", and is attributable to the presence of bats.

These biocorrosion processes have been the subject of several cave studies, first in tropical environments [7]-[12], then in Europe [6] [13]-[16], and in dry regions [17] [18].

These studies have demonstrated the existence of a specific late speleogenesis stage that is directly linked to the climatological and biological dynamics that accompany regional environmental changes. Biocorrosion, due to the long-term presence of bat colonies, results from the current or past occupation of large bat colonies in caves. It occurs in a late phase after the cave has been abandoned by active underground flow, but can reach a similar or even greater scale than the

initial development phase [8] [16] [18].

The articles cited above provide keys to understanding the features and mineralogy associated with this late stage speleogenesis. Although it has been possible to assess the extent of ablation rate due to biocorrosion in a few rare examples (**Table 1**), it is difficult to assess the actual rate of these biocorrosion processes, for several reasons. We do not know how long bats have inhabited the site, or how often they have been present, whether seasonally or over different periods of the Quaternary. Different species may be present on the same site for different uses, which will lead to various processes and intensities within the cave. For example, it is easy to understand why a hibernation site, where breathing, temperature and guano production are very modest, is much less affected than a nursery where bats are in full activity. Finally, are the populations present today representative of those of the past? For many sites, probably not. In fact, ablation rate rates calculated over the long term inevitably include phases where biocorrosion slows down or stops. These averages imply that the actual rates of wall retreat over short active periods are undoubtedly much higher.

However, various authors have tried to estimate long-term ablation rates that do not consider the short-term variations mentioned above. They propose values that can range between 0.4 and 40 mm/ka, depending on the context (**Table 1**).

Table 1. Long-term biocorrosion ablation rates proposed by various authors.

Reference	[19]	[7]	[8]	[9]	[14]	Audra *et al*., Chameau Cave, unpubl.	[16]
Average rate (mm/ka)	0.4	12	3 - 5	12.5	20 - 40	1	3 - 7
Maximum rate (mm/ka)			34	24			34

It is important to distinguish between the impact of biocorrosion linked to the aerosols released by the presence of bats and their guano, and that linked to the leachates that flow under the guano. For species that congregate in large colonies, particularly during the nursery periods, there can be significant accumulations of guano on the floor. This floor may correspond to the host limestone, to calcite speleothems, but also to detrital sediments which will also be impacted, including the artifacts they contain [16] [20] [21]. In addition to the floor, guano also accumulates on the wall ledges.

The decay of guano produces carbon dioxide, sulfates, and nitrates. Leachates acidified by carbonic, phosphoric, and sulfuric acids will flow out, responsible for the corrosion and weathering of carbonates and speleothems on the ground [22], with the correlative formation of specific mineralizations, mainly phosphates [23]. These aspects of limestone weathering are not confined to caves. Buildings and engineering structures also serve as habitats for bat colonies. They are subject to the same weathering processes. Depending on their type, they may be totally

affected (underground passages, underground quarries, cellars, etc.) or only partially (attics of castles or places of worship, etc.). In addition to limestone, biocorrosion by bat guano can also affect other building rocks such as feldspathic graywacke [24] or sandstone [25].

An eloquent example of monuments is Mohamed Ali's palace in Suez (Egypt). This building, constructed in 1812, was used until 1980, when it was abandoned. Bats then occupied some of the rooms, particularly the large dome. Bakr & Abd El Hafez [26] show how biocorrosion alters building materials 30 years later.

Biocorrosion appears to be the largest threat to the conservation of cave wall paintings [6] [15] [27] [28], but also to monuments [24] [26] [29]. The damages caused can be so extensive that operations to "relocate" settlements have already been carried out [30].

The aerosols and climatological changes caused by the bat colonies lead to biocorrosion on the walls and ceilings. At the same time, accumulations of guano on the floor cause specific biocorrosion of the carbonate substrates on which they rest.

It is this biocorrosion under guano that we will be addressing here; that linked to aggressive aerosols, which responds to completely different mechanisms, will not be considered in this study. We propose new data on the ablation rate associated with biocorrosion of limestone covered with guano. To do this, we will conduct 1) parallel tests in cave and in the laboratory. After 2) checking that the biocorrosion process has indeed taken place, 3) we will quantify its rate under different temperature conditions and as a function of the petrographic properties of the limestones used. We will also make macro- and microscopic observations showing the evolution of the surface of the exposed limestone. Finally 4), we will show that the laboratory method can be used to rapidly quantify the impact of biocorrosion directly linked to guano exposure on different substrates, and that it provides a better understanding of the mechanisms linked to biocorrosion.

2. Materials and Methods

2.1. Materials

This study is a continuation of that carried out on the impact of biocorrosion in the Prehistoric cave of Azé in France [16] [31] [32]. For this reason, we selected four regional Jurassic limestones of various textures (oolithic, micritic, crinoid), for which we indicate the main petrographic properties from the literature. Each tablet covered an area of 0.01 m^2 (**Table 2**).

We also tested a fragment of broken speleothem collected in the Orgnac Cave (Ardèche) to assess the impact of corrosion on calcite speleothems. The guano used came from the Courtouphle Cave in the Ain department, as there is no recent accumulation in the Mâconnais. The Courtouphle Cave is located on the other side of the Saône valley in a comparable context (latitude, altitude, landscape, etc.). This cave is also frequented by the same species of chiropteran as those found in the prehistoric cave at Azé. This ensures good reproducibility of past conditions in the cave.

Table 2. Petrographic characteristics of the different limestones used to manufacture the tablets used to simulate biocorrosion (NF = French Standard). From these 4 limestone pieces numbered from 1 to 4, 8 tablets were made, each type of limestone tablet then being placed in the cave (G) or in a thermostatic bath in the laboratory (L), and numbered 1G and 1L, 2G and 2L, etc., respectively.

Limestone tablet no.	1	2	3	4
Geological stage	Callovian	Bathonian	Bathonian	Bajocian
Petrography	Oolithic	Micritic	Micritic	Crinoid limestone
Quarry site	Quarry Les Buis, Ladoix-de-Serrigny	Light Comblanchien	Comblanchien, Rocherons Quarry	Buxy
Reference	https://lithoscopect-mnc.com/calcaire/corton/6834/	https://lithoscopect-mnc.com/calcaire/comblanchien/6829/	https://www.lapierredorival.fr/nos-pierres/pierre-de-comblanchien-clair-p10.html	https://lithoscopect-mnc.com/calcaire/buxy-bayadere/5786/
Density (kg/m^3) [NF EN 1936]	2620	2670	2600	2650
Open porosity (%) [NF EN 1936]	2.8	0.9	0.5	2.5
Perpendicular capillarity C1 (g·m^{-2}·s$^{-1/2}$) [NF EN 772-11]	3	0.7	0.9	4

2.2. Description of Tests, Method

a) Moisture analysis: the collected guano was analyzed for moisture content using a Mettler-Toledo HG63 thermo-balance accurate to 1/10 of a percent, and dried for 2 h at 105˚C. The guano contained 66% water.

b) Phosphorus analysis: a sample was sent to the CESAR laboratory in Ceyzeriat, Ain, for analysis of total phosphorus. The analysis was carried out in accordance with standards NF ISO 11466, NF ISO 11466 and ICP AES assay: NF EN ISO 11885. After drying, the phosphorus content in the guano, was: 35.14 g/kg.

c) Suspension preparation: to obtain a suspension, the dry guano was then mixed with demineralized water using a Rayneri mixer, fitted with a Rushton turbine, at a speed of 3300 rpm for a period of 2 min. The ratio of guano to demineralized water used was 1/2. The pH of the suspension was 4.15 at the start of the tests.

d) Determining the mass of the tablets: the limestone tablets were weighed beforehand after drying for 2 h at 105˚C.

e) Exposure of tablets to guano suspension: all were immersed separately in the guano suspension in closed 1L flasks. The first series (1L, 2L, 3L, 4L) was placed in the laboratory in a 24L thermostatic bath at 80˚C for 174 days. These tests had to be stopped in March 2020 due to the pandemic confinement. A second series (1G, 2G, 3G, 4G) was also placed in the same suspension and in closed 1L flasks. They were placed in natural conditions in the Prehistoric cave of Azé for 789 days, at the roof of the "Grenier des Chauves-souris" (Bats cellar), an upward-sloping gallery used as a shelter by a colony of a few individuals present from spring to

autumn. In this place, the temperature varies between 11.0˚C in winter and 16.5˚C in summer. For the Orgnac Cave speleothem sample, it was possible to assess biocorrosion at 80˚C for only 55 days, also because of the pandemic.

2.3. Quantification of Biocorrosion

a) Changes in the weight of the tablets during exposure: before the tests and each time they were removed, the tablets corresponding to the different tested limestones were dried for 2 h at 105˚C, then weighed using a Mettler AB304-S/FACT balance accurate to 1/10,000 g. Those placed in the thermostatic bath (L series) were removed from it several times to observe their evolution.

b) Recovery of phosphate mineral crust: after drying for 2 h at 105˚C in a ventilated oven, they were scraped with a lanceolate spatula to remove the crust that had formed on their surface. This probably encourages biocorrosion by removing the insoluble layer of phosphate minerals that waterproof the limestone. The mineralogy of these crusts was then analyzed.

c) Guano exposure continues: once returned to their respective 1L flasks, the tablets were immediately immersed in the thermostatic bath.

2.4. Method Adaptation

The limestone and guano were chosen to be representative of the regional context of the Azé cave. Naturally, the choices will have to be adapted to suit the subjects under study. The limestones and guanos chosen will have to be defined for each case.

2.5. Mineralogy

Mineral identification was carried out by X-ray diffraction (XRD) using a Rigaku RU-200BH X-ray generator equipped with a rotating anode, an Osmic multilayer optic, and a mar345 2D detector. The wavelength used was that of Cu, $\lambda = 0.15418$ nm, and the applied power was 50 kV and 50 mA. The samples were finely ground, the obtained powder was homogenized, and then placed in a glass capillary 0.5 mm in diameter. The volume of powder exposed to the X-rays for each measurement was around 0.1 µl.

2.6. Observation of Tablets

Changes in mineralogy lead to variations in tablet color. Those in the L series, immersed at 80˚C, were qualified using a Fru WR10-8MM colorimeter in the L, a, b system. The values were averaged from 5 measurements. Tablets were observed visually. They were systematically photographed using an Olympus Tough F2.0 camera. At the end of the tests, the tablets were observed using a low and high-resolution micrograph; images were acquired with a scanning electron microscope (SEM) JEOL JSM-6340F at 5 and 15 kV. Energy dispersive X-ray spectroscopy (EDX) elemental analyses were carried out in selected areas of the different places observed in SEM at 15 kV (Si-Li detector, Quantax, Brucker AXS Microanalysis GmbH Berlin, Germany). The samples were cut into pieces of 20 × 20 mm^2 and covered with

carbon to evacuate the electrical charges.

2.7. Evolution of the pH of the Guano Suspension

The pH was measured using a Mettler-Toledo Seven Excellence pH meter fitted with an Inlab-731-ISM electrode accurate to 1/100 pH unit. The values indicated are those corrected to a temperature of 25˚C.

3. Results

3.1. Quantification of biocorrosion

All tablets show a loss of mass (Table 3).

Table 3. Mass loss recorded on the tablets immersed in the guano suspension in the cave (G) and at 80˚C in the laboratory (L).

Sample no.	Duration of experiment (days)	Loss of mass (g)	Loss of mass (%)	Standardized loss of mass (%/year)
1G	789	0.47	0.52	0.24
2G	789	0.42	0.37	0.17
3G	789	0.32	0.28	0.13
4G	789	0.24	0.24	0.11
1L	174	4.12	4.59	9.6
2L	174	/	/	/
3L	174	3.42	3.47	7.3
4L	174	2.51	2.71	5.7

For the L series immersed in the guano suspension at 80˚C, the measured mass losses appear to vary linearly with time (Figure 1). Except for plate no. 2L, which experienced a slight loss of mass for the first 48 days, but remained stable for the rest of the experiment.

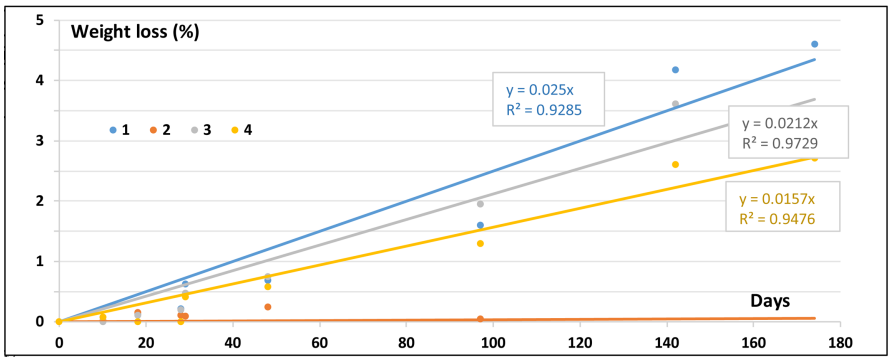

Figure 1. Changes over time in the mass loss of limestone tablets immersed in the guano suspension at 80˚C. 1L, 2L, 3L, and 4L refer to tablets corresponding to limestones 1, 2, 3, and 4 respectively (Table 1).

Based on the mass losses of the tablets, it is possible to extrapolate the theoretical time required for a mass loss of 2.5% under the conditions of exposure at constant ambient temperature in the cave. The results are 11 years for the 1G and 2G samples, 15 years for 3G, and 24 years for 4G.

If we consider a surface exposed in the cave to the same guano suspension, it will take between 279 and 613 years for this surface to retreat by 2.5 mm. The rate would then be between 0.004 and 0.008 mm/year, values calculated for the Azé Cave for the current temperature, which is between 11.0˚C and 16.5˚C.

With the same limestones, at 80˚C, it would take only 8 to 13 years to reach this retreat of 2.5 mm, and the rate of retreat would then be between 0.20 and 0.32 mm/year, *i.e.* an ablation rate around 35 to 50 times greater than that obtained at the ambient temperature of the cave.

Unfortunately, reproducibility tests could not be carried out because of the pandemic.

3.2. Mineralogy

The crusts collected during each measurement were analyzed by XRD (Table 4).

Table 4. Phosphate minerals present in crusts from L-series tablets exposed to guano suspension at 80˚C. The values given in the "Magnesian Whitlockite" column are the mass percentages obtained from a semi-quantitative analysis. For other minerals, an X indicates their presence.

Reference		Magnesian whitlockite $Ca_9Mg(HPO_4)(PO_4)_6$ (% of mass)	Hydroxylapatite $Ca_{10}(PO_4)_6(OH)_2$	Monetite $CaHPO_4$
Sample	1L	81		
	2L	58	X	
	3L	68	X	
	4L	90		X

3.3. Tablets and Speleothem Evolution

We observed the formation of crusts on tablets from the L series immersed in the suspension at 80˚C (Figure 2). No visual changes were observed on tablet 2.

After exposure to guano in the laboratory, the color of the platelets changed, as shown by the measured L, a, b values, going from grey to brown (Table 5).

The tablets subjected to the hot test in the laboratory and after scraping showed the following macroscopic changes (Figure 2):

- Tablet 1L: appearance of depressed areas up to 1 mm deep;
- Tablet 2L: a few rare areas appear with an indented micro-relief;
- Tablet 3L: the weathering marks the micritic cement of the limestone (Figure 3). A small part of the tablet shows a depression about 0.5 mm deep;
- Tablet 4L: appearance of depressed areas up to 1 mm deep over most of the surface of the tablet.

On the tablet of sample 3, visually the corrosion mechanism is the same in the hot experiment (3L) and in the cave (3G). It occurs to the detriment of the micritic cement of the limestone, sparing the sparite crystals (**Figure 3**). This mechanism is the same as that shown by Zupan-Hajna [33] for limestone weathering phenomena linked to corrosion by moisture flowing down along cave walls.

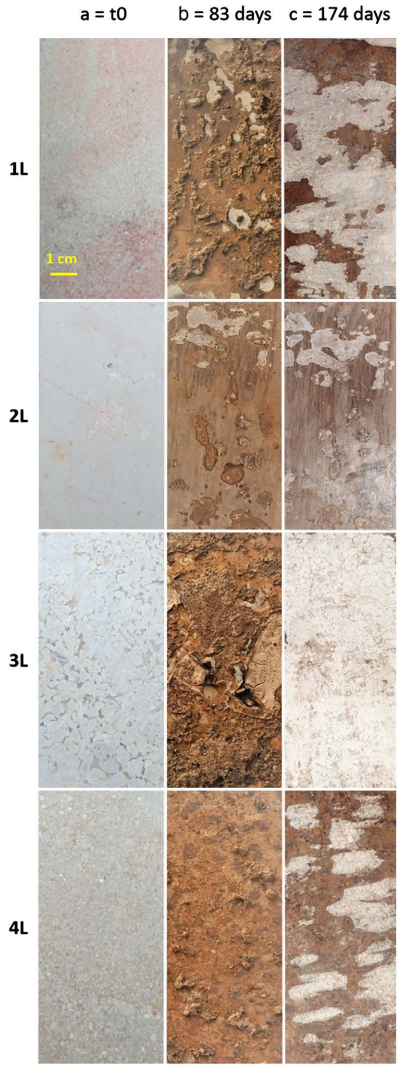

Figure 2. Macroscopic changes in L-series tablets in guano suspension at 80˚C. Lines 1L, 2L, 3L, 4L correspond to each limestone sample, the columns show the evolution at a = T0 (before immersion), b = after 83 days and before scraping, and c = after 174 days and after scraping.

Table 5. Changes in platelet color before and after exposure to guano suspension in the laboratory (colorimetry using the L, a, b measurement system).

Sample	1L	2L	3L	4L
Initial color	63.37/8.82/7.21	68.40/7.52/0.31	72.76/6.14/3.58	60.57/7.84/6.44
Color after laboratory experiment	34.33/10.52/12.42	47.88/6.45/3.27	44.89/9.51/12.74	40.18/8.68/10.86

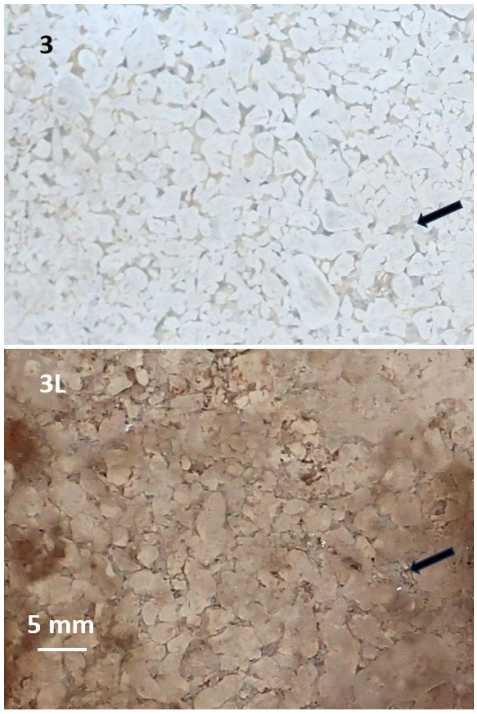

Figure 3. Upper part: 3 = sample 3 = unexposed tablet; lower part: 3L = sample 3 tablet exposed at 80˚C. For the same limestone, in both cases the micritic cement (arrow) appears to be the weathered part of the limestone, the sparite crystals being visually unaffected.

We were able to observe the same mechanism on the speleothem subjected to guano suspension for 55 days at high temperature. When it was removed from suspension, it partially disintegrated into large sparite crystals (**Figure 4**), and the joins separating the crystals appear to be the most altered zones.

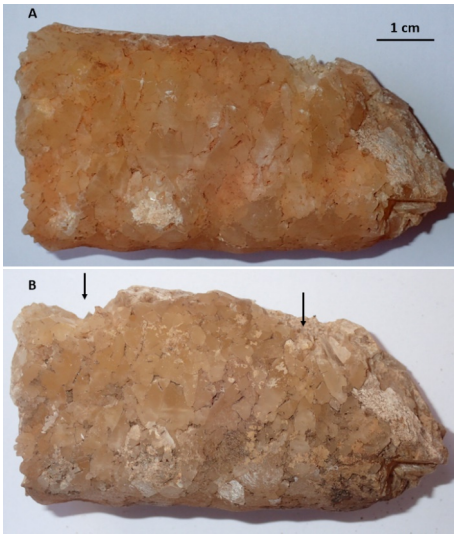

Figure 4. Evolution of a speleothem from Orgnac Cave after 55 days in guano suspension at 80˚C, A: before experiment, B: after immersion in guano suspension. Sparite crystals have been dissociated by intercrystalline dissolution. The arrows indicate areas where the sparite crystals broke up during scraping.

In the SEM, for tablets exposed to the bath at 80˚C (1L, 2L, 3L, 4L), fairly compact crusts and spherical structures on the order of one micron are generally observed. Corrosion pits are visible on the calcite crystals. Inside the pits, spherical crystals have appeared such as for the tablet 4 (Figure 5).

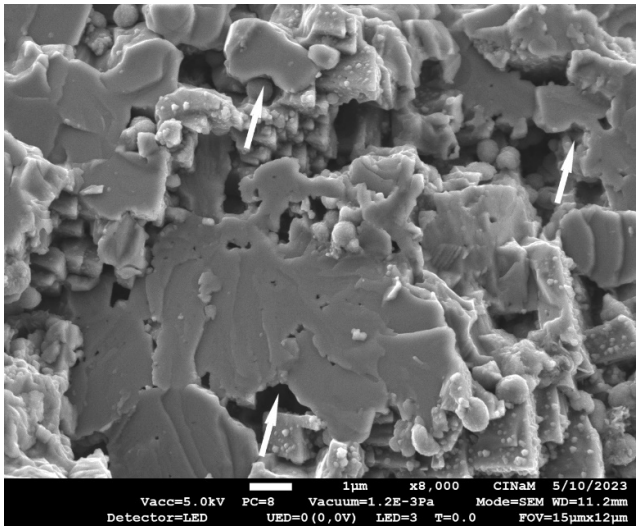

Figure 5. SEM image of 4L tablet. Corrosion gulfs are visible on the calcite crystals, containing spherical crystals.

Chemical analyses by EDX systematically indicate (apart from C and O): Ca, P, Mg and quite often S and Si-Al (Si and Al probably come from the clays, detected in small quantities by DRX, plates 1L and 4L). Chemical analysis of spherical particles on tablet 1L for example (Figure 6) shows a composition rich in Ca, P and Mg (Figure 7). These analyses indicate that the spheres are very probably whitlockite, in agreement with the phases identified by XRD (whitlockite + calcite from the host rock).

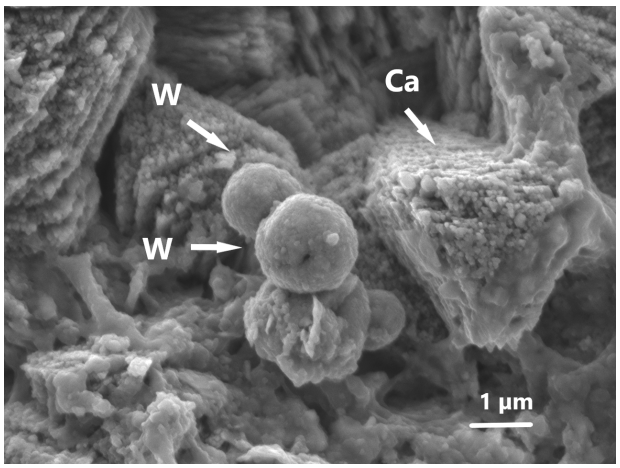

Figure 6. High-resolution SEM image on tablet 1L, with arrows showing the zones analyzed by EDX. W = whitlockite; Ca = calcite, where cleavages appear to be etched. The areas analyzed are around 5 µm for the voltage used, 15 kV and this chemical composition.

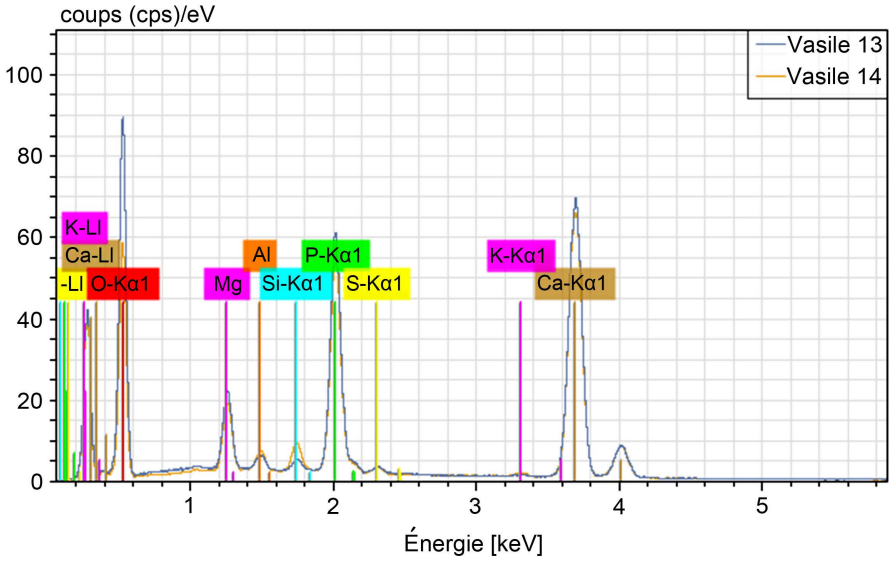

Figure 7. Results of EDX chemical analysis of tablet 1L, carried out at the points shown in **Figure 6**.

For tablets exposed to guano in caves (1G, 2G, 3G, 4G), very few crusts and few spherical structures were generally observed. Chemical analysis by EDX shows the systematic presence (apart from C and O) of: Ca, Mg, quite often Si-Al, and rarely S. On tablet 4G, we found P in one of the analysis points, which tends to confirm the possible presence of the brushite indicated by DRX.

Comparison of the SEM images obtained after exposure of sample 4 in the cave and in the laboratory shows the evolution in the size of the whitlockite crystals (**Figure 8**). After 789 days in the cave, the whitlockite crystals that formed measured around 10 nm in diameter (**Figure 8(A)**). After 174 days in the laboratory at 80˚C, spheres around 900 nm in size can be seen associated with smaller crystals (**Figure 8(B)** and **Figure 8(C)**). These spheres have a framboidal structure (**Figure 8(C)** and **Figure 9**), showing that agglomeration of the primary structures is responsible for their growth.

Figure 8. limestone sample 4. The white bar in the legend is 1 µm long. A: after 789 days in the cave; B and C: after 174 days at 80˚C in the laboratory; C: detail of framboidal crystals obtained by agglomeration of primary structures. Arrows indicate spheres of whitlockite gradually growing.

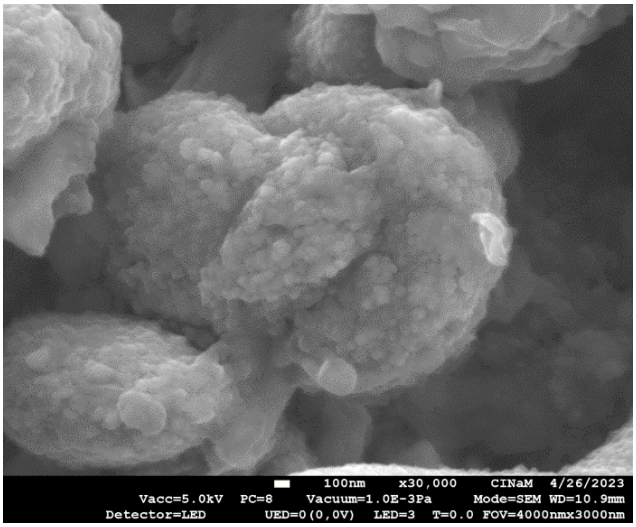

Figure 9. Framboidal structure of whitlockite formed by agglomeration of primary crystals.

3.4. Evolution of the pH of the Guano Suspension

The pH of the guano suspension was 4.15 at the start of the tests.

For the tests carried out in the laboratory at 80˚C, the pH rose slightly to 4.42 after 30 days. We were unable to measure this at the end of the tests because of the shutdown imposed by the first lockdown. For the tests carried out in caves at ambient temperature, the pH of the suspension rose to 6.66 at the end of the exposure time (789 days).

4. Discussion

The hot tests confirmed that a crust of phosphate minerals formed on the surface of the tablets, by epigenesis of the carbonates reacting with the phosphoric acid contained in the guano suspension. Hydroxylapatite was formed in two of the samples by the chemical reaction (1):

$$\begin{aligned} &5CaCO_3\left[\text{calcite}\right]+3H_2PO_4^-\left[\text{phosphoric acid}\right] \\ &\rightarrow Ca_5\left(PO_4\right)_3\left(OH\right)\left[\text{hydroxylapatite}\right]+H_2O+3HCO_3^-+2CO_2 \end{aligned} \quad (1)$$

The outgassing of CO_2 resulted in a "swelling" of the flasks while they were in the thermostatic bath. Hydroxylapatite is not formed directly, but via the formation of an intermediate phosphate, brushite, as a result of the chemical reaction between phosphoric acid and ammonia, which is also present in the guano, according to reactions (2) and (3).

$$2NH_3+H_3PO_4\rightarrow\left(NH_4\right)_2\left(PO_3OH\right) \quad (2)$$

$$\left(NH_4\right)_2\left(PO_3OH\right)+Ca^{2+}+2H_2O\rightarrow Ca\left(PO_3OH\right)\cdot 2H_2O\left[\text{Brushite}\right]+2NH_4^+ \quad (3)$$

The ammonium formed, which is highly soluble, was not found in our analyses because it was probably leached out during tablet washing.

We mainly obtained the formation of whitlockite [$Ca_9Mg(HPO_4)(PO_4)_6$], which is a calcium and magnesium phosphate. These last two elements come from

limestone. Whitlockite is formed by the substitution of calcium for magnesium from calcium phosphates, and in particular from hydroxylapatite and brushite. This substitution is favored by time and temperature and takes place at 80˚C in only 12 hours [34]-[36]. Our SEM observations show that the crystals initially formed measure around 10 nm. They then bundle together to form increasingly large agglomerates that will eventually form a crust on the surface of the limestone tablets.

The presence of monetite is probably linked to a secondary reaction (4). This is generally derived from the dehydration of brushite after its formation in the reaction medium [37] [38] according to:

$$\mathrm{Ca}\left(\mathrm{PO_3OH}\right)\cdot 2\mathrm{H_2O} \rightarrow \mathrm{Ca}\left(\mathrm{PO_3OH}\right)\left[\text{monetite}\right] + 2\mathrm{H_2O} \quad (4)$$

It could occur during the drying of the tablets at 105˚C before weighing and recovery of the crusts [39] [40], and can therefore be considered as a possible operating artifact.

The formation of phosphate minerals associated with guano therefore depends on time and environmental conditions, whether in karstic caves or in the laboratory [18] [23]. This phosphatisation is accompanied by an acidification of the pH of the guano, a change in the color of the bedrock towards brown, and the appearance of a corroded surface.

Our macroscopic observations show that the acid leachate from the guano acts primarily on the micrite that cements the limestone. The attack takes place preferentially along the joins separating the crystals, whether in limestone or within a speleothem.

The tablets we used were taken from limestones with different physical properties of porosity and capillarity (**Table 2**).

Sample 1 has both high porosity and high capillarity. It has been weathered the most and has the highest rate of ablation. Only whitlockite was determined, showing that the phosphate minerals had all had time to evolve into this stable species.

Sample 2, which has both low porosity and small pore sizes, was virtually not weathered, even when hot.

Sample 3 has low porosity but higher capillarity than sample 2. It also has calcite crystals that are clearly visible to the naked eye, which is not the case for the other samples. These two characteristics are probably responsible for the much greater loss of mass in this sample than in sample 2. Capillarity would therefore allow better diffusion of the fluid within the tablet. The size of the sparite crystals may mean that they offer a surface that is more easily accessible to phosphoric acid due to preferential weathering along the interfaces between crystals. In both samples, hydroxylapatite and whitlockite are present. This could reflect slower phosphate-calcium reactions due to reduced fluid circulation in the capillary structure of the rock. It would then be the size of the calcite crystals that would favor their weathering and generate a greater rate of ablation, firstly by inter-granular dissolution, then by disintegration of the sparite grains.

Sample 4, like sample 1, has both high porosity and capillarity. Although its ablation rate is slightly lower than that of sample 1, the characteristics associated with its ablation and the associated mineralogy are similar. The presence of monetite is likely to be an artifact of laboratory manipulation.

According to these results, several limestone characteristics may or may not favor biocorrosion:

- Porosity: the higher the porosity, the higher the quantity of phosphoric acid impregnating the limestone;

- Capillarity: for rocks with a low pore volume, this characteristic is of prime importance. It will determine whether or not the fluid can enter the limestone and circulate more or less quickly;

- The size of the calcite crystals: it is likely that the larger the size, the more the calcite will be exposed to corrosion through the formation of preferential paths for the fluid between the boundaries of crystals. This could be due to the fact that in the initial limestone, the inter-crystalline boundaries between the large crystals are more open than those between the small crystals.

These characteristics are important for setting up biocorrosion processes, as they will promote chemical reactions by controlling the circulation and quantity of corrosive fluids in the limestone weathering front.

We show that temperature has a direct influence on the rate of weathering. During its evolution, guano undergoes a temperature increase linked to its fermentation. Unfortunately, we have no data on the temperature for guano piles in the Mâconnais region, as there is currently no large colony of bats there, and it would appear that this has never been documented elsewhere. However, during the decay of organic matter by composting, the maximum temperature of accumulation can reach between 45˚C and 80˚C depending on the biodegradability of the material [41]. The hot tests we carried out correspond to this maximum potential temperature. They are therefore probably representative of biocorrosion pushed to the extreme under a large accumulation of guano, which could very well be the case in tropical cavities or in Egypt, in a monument built in an arid zone but where generally the underground environment and the temples are often saturated with humidity, which favors mineralization.

The presence of a colony of bats leads to a significant change in the aerology of the cave. This is the origin of condensation phenomena in an intermediate zone between the accumulation of guano on the floor and the swarms on the ceiling, as has been shown at Espalungue [42]. This condensation helps to produce the water that will leach the guano and accelerate its mineralization.

For the most porous limestone, when hot, after 174 days, mass loss is around 4.5%. We have therefore shown that, under extreme conditions, weathering can be very rapid, whether on the wall, on the floor, or for any lithic element in sediments, when the combination of conditions is favorable: fresh and renewed guano, a water supply that allows acid leachates to be obtained, and regular leaching of the weathered rock. In a cave, the rate of ablation of a wall can vary between

0.004 and 0.008 mm/year, *i.e.* 4 to 8 mm/ka, for a cave where the temperature ranges between 11.0˚C and 16.5˚C. The effect of biocorrosion is greatly enhanced by temperature, and thus at a temperature of 80˚C the rate of ablation rises to 20 to 32 cm/ka (*i.e.* 35 to 50 times more), theoretical orders of magnitude that could perhaps be achieved under certain conditions for buildings constructed with limestone in hot regions.

These values confirm that biocorrosion caused by bats can have a catastrophic effect on cultural heritage, as demonstrated by the Mohamed Ali monument in Suez, where the coatings supporting the frescoes were degraded in less than 30 years. In addition, a micro-topographic study of the walls bearing various engravings in the nearby Agneux I Cave [43], Saône-et-Loire, France, shows that the depth of the engravings is between 0.07 and 0.2 mm. If they were covered by guano, it would take between 9 and 50 years for them to be completely erased! The same applies to all the bioglyphs left by prehistoric animals, such as cave bear scratches [44]. In just a few years, they can be erased by biocorrosion.

5. Conclusions

The tests carried out show the impact of guanos on different limestones. Limestone characteristics (composition, type of calcium carbonate crystals, porosity) appear to be the key factors in determining its resistance to biocorrosion. We demonstrated selective dissolution of calcium carbonate affecting micrite before sparite. Calcium carbonate is replaced by a phosphate (whitlockite). The resulting crystals grow to form framboidal structures. This corrosion leads to the formation of crusts on the limestone surface, which can be removed mechanically. Mass loss can reach 4.5% in 174 days at 80˚C.

The tests we have carried out in the Prehistoric cave of Azé and in the laboratory show that the biocorrosion mechanisms are similar in both environments. The conditions defined here can therefore be used to measure the ability of a material to resist or not to biocorrosion caused by bat guano. This test makes it possible to evaluate in the same (very short) time, the ability of many materials to be affected by biocorrosion. The samples tested are subjected to the same guano under the same conditions, enabling a direct comparison. The conditions defined here lead to an acceleration of biocorrosion by at least 50 times, providing a rapid response in a controlled environment.

In the future, this test protocol will also provide a better understanding of the mechanisms that cause biocorrosion, particularly those related to its diffusion within a material that has not yet been weathered, mechanisms that are still largely unknown today. It will also provide a quantitative and qualitative basis for modeling these processes in various contexts.

This is already helping to explain the crystallization processes that lead to the formation of whitlockite crusts. We show the weathering of calcite crystals caused by phosphoric acid corrosion. The reaction between calcium and phosphoric acid first leads to the formation of brushite, which then evolves into hydroxylapatite.

Substituting magnesium for calcium produces whitlockite. The initial crystals measure around 10 nm and are located in the gulfs created by the corrosion of calcite crystals. They then cover the calcite and grow by bundling to form larger agglomerates which ultimately form the crust covering the limestone.

Since the discovery of bat-related biocorrosion in karst, several authors have tried to assess its impact by estimating the rate of wall ablation. However, only aerosol-related biocorrosion was considered, with a maximum value of 40 mm/year. Here we present new data on the rate of ablation of walls or floors directly exposed to guano, with a maximum value of 8 mm/ka.

For a building exposed to high temperatures, as is the case in Egypt, the ablation rate can reach several decimeters per millennium (320 mm/ka measured during this study). While it is difficult to set nature against culture, for endangered monuments this inevitably means protection of stones against guano accumulation and regular cleaning of surfaces exposed to guanos in order to preserve them.

This value shows that an engraving made on a limestone conducive to biocorrosion can be "erased" in just a few decades if it is covered by a large quantity of guano leached by dripping. This is the case, for example, of the Great Pillar of the Great Chamber in the Isturitz cave [14] [45], where the engravings that covered it were partly preserved from biocorrosion after being buried under sediments. This phenomenon affects the morphology of the galleries and the carbonates of cave sediments, as well as the paleontological material (bones) and the cave art, both prehistoric and more recent. Biocorrosion caused by bat guanos can lead to the deterioration in just a few years of many man-made features, in particular historic monuments, but also all the traces left by animals in a cave and archaeological artefacts (bones, ceramics, lithic industry).

In the future, this method will make it possible to select the most suitable materials to resist biocorrosion, whether for the renovation of cultural heritage or the construction of new buildings that could be subjected to guanos of various origins (pigeon droppings, for example).

Highlights

- Bat guanos have a significant impact on the weathering of monuments and caves.

- We develop a method for rapidly measuring this impact.

- We show that this impact depends not only on the nature and properties of the limestone, but also on the environmental conditions in which the limestone is exposed to guano.

- We discuss the mechanisms behind this biocorrosion.

Acknowledgements

We would like to thank Frédéric Thomasset for preparing and supplying the limestone tablets and Yves Contet for collecting and supplying the guano. We would also like to thank the Saône-et-Loire Departmental Council for allowing us to

carry out research at the Azé caves.

Funding

Association for Research and Valorization of the Azé Caves and the Mâconnais-Clunisois.

Authors' Contributions

BL, setting up the study, carrying it out, interpreting and writing; HV: DRX and interpreting writing; GO: SEM and EDX and interpreting; AP, BL and DC: interpreting and writing.

Conflicts of Interest

The authors declare that they have no known competing financial interests or personal relationships that could have appeared to influence the work reported in this paper.

References

[1] Breuil (1950) Lascaux. *Bulletin de la Société préhistorique de France*, **47**, 355-363. https://doi.org/10.3406/bspf.1950.2712

[2] Cosquer, H. (1992) La grotte Cosquer, plongée dans la préhistoire. Ed. Solar.

[3] Collina-Girard, J. (1996) Préhistoire et karst littoral: La grotte Cosquer et les Calanques marseillaises (Bouches-du-Rhône, France). *Karstologia*: *Revue de karstologie et de spéléologie physique*, **27**, 27-40. https://doi.org/10.3406/karst.1996.2363

[4] Chauvet, J.M., Brunel Deschamps, E. and Hillaire, C. (1995) La grotte Chauvet à Vallon-Pont-d'Arc. Seuil.

[5] Delannoy, J., Sadier, B., Jaillet, S., Ployon, E. and Geneste, J. (2010) Reconstitution de l'entrée préhistorique de la grotte Chauvet-Pont d'Arc (Ardèche, France): Les apports de l'analyse géomorphologique et de la modélisation 3D. *Karstologia*: *Revue de karstologie et de spéléologie physique*, **56**, 17-34. https://doi.org/10.3406/karst.2010.2679

[6] Gély, B., Cailhol, D., Clottes, J., Traian Lascu, V., Le Guillou, Y., *et al*. (2018) Peştera Coliboaia (Campani, Bihor) grotte ornée aurignacienne de Roumanie. État d'avancement des études pluridisciplinaires (2009-2014). *XIXe International Rock Art Conference IFRAO*, Cáceres, July 2015, 161-189.

[7] Lundberg, J. and McFarlane, D.A. (2009) Bats and Bell Holes: The Microclimatic Impact of Bat Roosting, Using a Case Study from Runaway Bay Caves, Jamaica. *Geomorphology*, **106**, 78-85. https://doi.org/10.1016/j.geomorph.2008.09.022

[8] Lundberg, J. and McFarlane, D.A. (2012) Post-Speleogenetic Biogenic Modification of Gomantong Caves, Sabah, Borneo. *Geomorphology*, **157**, 153-168. https://doi.org/10.1016/j.geomorph.2011.04.043

[9] Lundberg, J. and McFarlane, D.A. (2015) Microclimate and Niche Constructionism in Tropical Bat Caves: A Case Study from Mount Elgon, Kenya. In: Feinberg, J., Gao, Y. and Alexander, E.C., Eds., *Caves and Karst across Time*, Geological Society of America Special Paper, 211-229.

[10] Bigot, J.Y. and Guyot, J.L. (2013) Chauves-souris et condensation-corrosion dans les grottes du Pérou. Actes de la vingt-troisième Rencontre d'Octobre, Le Châtelard,

2014, 22-27.

[11] Audra, P., Bosák, P., Gázquez, F., Cailhol, D., Skála, R., Lisá, L., *et al*. (2017) Bat Urea-Derived Minerals in Arid Environment. First Identification of Allantoin, $C_4H_6N_4O_3$, in Kahf Kharrat Najem Cave, United Arab Emirates. *International Journal of Speleology*, **46**, 81-92. https://doi.org/10.5038/1827-806x.46.1.2001

[12] Dandurand, G., Duranthon, F., Jarry, M., Stratford, D.J. and Bruxelles, L. (2019) Biogenic Corrosion Caused by Bats in Drotsky's Cave (the Gcwihaba Hills, NW Botswana). *Geomorphology*, **327**, 284-296. https://doi.org/10.1016/j.geomorph.2018.10.027

[13] Bigot, J.Y. (2014) La corrosion pariétale des grottes par les aérosols d'origine animale. Actes de la vingt-troisième Rencontre d'Octobre, Le Châtelard, 2013; 14-21.

[14] Audra, P., Barriquand. L., Bigot, J.Y., Cailhol, C., Caillaud, H., Vanara, N., Nobécourt, J.C., Madonia, G., Vattano, M. and Renda, M. (2016) L'impact méconnu des chauvessouris et du guano dans l'évolution morphologique tardive des cavernes. Karstologia. https://hal.archives-ouvertes.fr/hal-01838348/document

[15] Bruxelles, L., Jarry, M., Bigot, J.Y., Bon, F., Cailhol, C., Dandurand, G. and Pallier, C. (2016) La biocorrosion, un nouveau paramètre à prendre en compte pour interpréter la répartition des œuvres pariétales: l'exemple de la grotte du Mas d'Azil en Ariège. Karstologia. https://hal.archives-ouvertes.fr/hal-01838098/document

[16] Barriquand, L., Bigot, J., Audra, P., Cailhol, D., Gauchon, C., Heresanu, V., *et al*. (2021) Caves and Bats: Morphological Impacts and Archaeological Implications. The Azé Prehistoric Cave (saône-Et-Loire, France). *Geomorphology*, **388**, Article ID: 107785. https://doi.org/10.1016/j.geomorph.2021.107785

[17] Frumkin, A., Aharon, S., Davidovich, U., Langford, B., Negev, Y., Ullman, M., *et al*. (2018) Old and Recent Processes in a Warm and Humid Desert Hypogene Cave: 'a'rak Na'asane, Israel. *International Journal of Speleology*, **47**, 307-321. https://doi.org/10.5038/1827-806x.47.3.2178

[18] Audra, P., Heresanu, V., Barriquand, L., El Kadiri Boutchich, M., Jaillet, S., Pons-Branchu, E., *et al*. (2021) Bat Guano Minerals and Mineralization Processes in Chameau Cave, Eastern Morocco. *International Journal of Speleology*, **50**, 91-109. https://doi.org/10.5038/1827-806x.50.1.2374

[19] Auler, A.S. and Smart, P.L. (2004) Rates of Condensation Corrosion in Speleothems of Semi-Arid Northeastern Brazil. Speleogenesis and Evolution of Karst Aquifers. https://www.researchgate.net/publication/26448068_Rates_of_condensation_corrosion_in_speleothems_of_semi-arid_northeastern_Brazil

[20] Shahack-Gross, R., Berna, F., Karkanas, P. and Weiner, S. (2004) Bat Guano and Preservation of Archaeological Remains in Cave Sites. *Journal of Archaeological Science*, **31**, 1259-1272. https://doi.org/10.1016/j.jas.2004.02.004

[21] Hoellinger, S. (2023) Taphonomie des niveaux moustériens de la grotte de Gatzarria: La piste de la biocorrosion, analyses géochimiques des résidus à la surface de vestiges lithiques. MSc Thesis, Histoire, Arts et Archéologie, Université Toulouse Jean-Jaurès.

[22] De Lumley, H., Fontaneil, C., Mestour, B., Perrenoud, C. and Saos, T. (2020) Caune de l'Arago, Tautavel-en-Roussillon, Pyrénées-Orientales, France, III, Etudes granulométrique, pétrographique, minéralogique, géochimique, micromorphologique et de la susceptibilité magnétique des formations pléistocènes de la Caune de l'Arago et de son environnement géologique. CNRS Editions; 373-560.

[23] Audra, P., De Waele, J., Bentaleb, I., Chroňáková, A., Krištůfek, V., D'Angeli, I., *et al*. (2019) Guano-Related Phosphate-Rich Minerals in European Caves. *International Journal of Speleology*, **48**, 75-105. https://doi.org/10.5038/1827-806x.48.1.2252

[24] Siedel, H., Plehwe-Leisen, E.V. and Leisen, H. (2008) Salt Load and Deterioration of Sandstone at the Temple of Angkor Wat, Cambodia. 11*th International Congress on Deterioration and Conservation of Stone*, Torun, Vol. 1, 267-274. http://elearn.hawk-hhg.de/projekte/salzwiki/media/E-Publication/Angkor_2008_Torun.pdf

[25] Hosono, T., Uchida, E., Suda, C., Ueno, A. and Nakagawa, T. (2006) Salt Weathering of Sandstone at the Angkor Monuments, Cambodia: Identification of the Origins of Salts Using Sulfur and Strontium Isotopes. *Journal of Archaeological Science*, **33**, 1541-1551. https://doi.org/10.1016/j.jas.2006.01.018

[26] Bakr, A. and Abd El Hafez, M. (2013) Role Assessment of Bat Excretions in Degradation of Painted Surface from Mohamed Ali's Palace, Suez, Egypt. *Egyptian Journal of Archaeological and Restoration Studies*, **3**, 47-56. https://doi.org/10.21608/ejars.2013.7447

[27] Caillaud, H. (2017) Zookarstologie: Les chiroptères comme facteurs géomorphologiques des paysages souterrains. Université Paris 1 Panthéon-Sorbonne, Mémoire de master 2 de géographie.

[28] Bruxelles, L., Barriquand, L., Beauvillier, M., Cailhol, D., Dardenne, E., Develle, A.L., Frouin, M., Galant, P., Galera, J.L., Genuite, K., Le Guillou, Y., Hoellinger, S., Jaillet, S., Kanievski, D., Lartiges, B., Le Roux, G., Otto, T., Pallier, C., Pisapia, C., Pfendler, S., Pons-Branchu, E., Touron, S. and Vanara, N. (2024) Biocorrosion et art pariétal: Une exclusion mutuelle à l'origine de vides archéologiques. Méthodologie, premiers résultats et nouvelles perspectives de recherche. *Bulletin de la société Préhistorique française*, *Actes du* 29*e congrès Préhistorique de France*, Toulouse, 31 mai au 4 juin 2021, 85-104.

[29] Yoshimura, S. and Kondo, J. (2004) Conservation of the Wall Paintings in the Royal Tomb of Amenophis III, First and Second Phases Report. Rapport, under the Auspices of UNESCO/Japan Trust Fund Joint Project of Supreme Council of Antiquities, Ministry of Culture Arab Republic of Egypt and Institute of Egyptology, Waseda University. https://unesdoc.unesco.org/ark:/48223/pf0000139296/PDF/139296eng.pdf.multi

[30] Porter, J.H. and Corda, K. (2013) Account of an Informed Bat Exclusion at the Temple of Deir El-Shelwit, Luxor, Egypt. *Conservation and Management of Archaeological Sites*, **15**, 195-212. https://doi.org/10.1179/1350503313z.00000000055

[31] Barriquand, L., Barriquand, J., Guillot, L., and Nykiel, C. (2011) Le site des grottes d'Azé. Le fruit de 60 ans de recherches dans le karst du massif de Rochebin (Saône-et-Loire). Spelunca. https://www.researchgate.net/publication/317825222

[32] Barriquand, L., Barriquand, J., Argant, A., Floss, H., Gallay, A., Guérin, C., Guillot, L., Jeannet, M., Nykiel, C. and Quinif, Y. (2011) Le site des Grottes d'Azé. Qua-ternaire. https://www.researchgate.net/publication/287600846

[33] Zupan Hajna, N. (2003) Incomplete Solution: Weathering of Cave Walls and the Production, Transport and Deposition of Carbonate Fines. ZRC SAZU, Založba ZRC, 168 p. https://doi.org/10.3986/9616358855

[34] Tas, A.C. (2016) Transformation of Brushite ($CaHPO_4{\cdot}2H_2O$) to Whitlockite ($Ca_9Mg(HPO_4)(PO_4)_6$) or Other Caps in Physiologically Relevant Solutions. *Journal of the American Ceramic Society*, **99**, 1200-1206. https://doi.org/10.1111/jace.14069

[35] Kizalaite, A., Grigoraviciute-Puroniene, I., Asuigui, D.R.C., Stoll, S.L., Cho, S.H., Sekino, T., *et al.* (2021) Dissolution-Precipitation Synthesis and Characterization of Zinc Whitlockite with Variable Metal Content. *ACS Biomaterials Science & Engineering*, **7**, 3586-3593. https://doi.org/10.1021/acsbiomaterials.1c00335

[36] Jang, H.L., Lee, H.K., Jin, K., Ahn, H., Lee, H. and Nam, K.T. (2015) Phase Transformation from Hydroxyapatite to the Secondary Bone Mineral, Whitlockite. *Journal of Materials Chemistry B*, **3**, 1342-1349. https://doi.org/10.1039/c4tb01793e

[37] Frost, R.L. and Palmer, S.J. (2011) Thermal Stability of the "Cave" Mineral Brushite $CaHPO_4{\cdot}2H_2O$—Mechanism of Formation and Decomposition. *Thermochimica Acta*, **521**, 14-17. https://doi.org/10.1016/j.tca.2011.03.035

[38] Dumitraș, D. and Marincea, Ș. (2021) Sequential Dehydration of the Phosphate-Sulfate Association from Gura Dobrogei Cave, Dobrogea, Romania. *European Journal of Mineralogy*, **33**, 329-340. https://doi.org/10.5194/ejm-33-329-2021

[39] de Schultén, M.A. (1901) Reproduction artificielle de la monétite. *Bulletin de la Société française de Minéralogie*, **24**, 323-326. https://doi.org/10.3406/bulmi.1901.2592

[40] de Schultén, M.A. (1903) Recherches sur le phosphate dicalcique. Reproduction artificielle de la brushite. Reproduction de la monétite par un nouveau procédé. *Bulletin de la Société française de Minéralogie*, **26**, 11-17. https://doi.org/10.3406/bulmi.1903.2666

[41] Mustin, M. (1987) Le compost: Gestion de la matière organique. Éditions François Dubusc.

[42] Cailhol, D., Delmasure, M.C., de Valicourt, E. and Vanara, N. (2018) Grotte d'Espalungue: Étude des processus de condensation-corrosion et de biocorrosion; guano et biodiversité. In Préhistoire ancienne de la vallée d'Ossau, Projet Collectif de Recherche, bilan 2018 et demande 2019-2021, laboratoire Traces; 44-51.

[43] Floss, H., Ruiz Lopez, J.F., Hoyer, C.T., Herkert, K., Huber, N., Rebentisch, A. and Rösch, A.M. (2018) Les figurations pariétales paléolithiques de la grotte Agneux I commune de Rully, Saône-et-Loire, France, une méthodologie de distinction entre préhistoire et modernité. In: Floss, H. and Pastoors, A., Eds., *Palaeolithic Rock and Cave Art in Central Europe*, Session 31 of the XIX International Rock Art Conference IFRAO 2015, Symbols in the Landscape: Rock Art and Its Context, Arkeos, 9-32.

[44] Bigot, J.Y., Audra, P., Bruxelles, L., Cailhol, D. and Pallier, C. (2023) Bear Claw Marks in Clay: Differential Conservation in Caves Harboring Bat Colonies. Mas d'Azil, Sirach and Lare caves, France. 18*th International Congress of Speleology*, Vol. 5, 335-338. https://www.researchgate.net/publication/364284366

[45] Garate Maidagan, D., Rivero, O., Labarge, A. and Normand, C. (2016) Le pilier gravé de la grotte d'Isturitz (Saint-Martin-d'Arberoue, Pyrénées-Atlantiques): Cent ans après sa découverte. *Bulletin de la Société Préhistorique Française*, **113**, 501-522. https://doi.org/10.3406/bspf.2016.14651